MEASUREMENT OF AURORAL ELECTRIC FIELDS WITH AN ANTARCTIC SOUNDING ROCKET S-310JA-7
2. AC ELECTRIC FIELD

Hisao YAMAGISHI, Hiroshi FUKUNISHI, Takeo HIRASAWA

National Institute of Polar Research, 9-10, Kaga 1-chome, Itabashi-ku, Tokyo 173

and

Toshio OGAWA

Geophysical Institute, Kyoto University, Kitashirakawa Oiwake-cho, Sakyo-ku, Kyoto 606

Abstract: A sounding rocket with double-probes for DC electric field and AC electric field (5–220 Hz band) measurement was launched from Syowa Station in Antarctica around the onset time of an intense auroral substorm. The rocket first encountered a poleward expanding auroral arc, where intense (1.4 mV/m) and broad band electric field fluctuations were measured around the arc at the altitude of 105–128 km. The rocket then moved across an equatorward drifting arc, where narrow-band electric field fluctuations around 40 Hz were measured at the altitude of ~190 km.

Considering the DC electric field data and the electron density gradient observed on the same rocket, it is likely that the former fluctuation is due to drift waves or ion acoustic waves excited by the cross-field type or two-stream type plasma instability, while the latter is due to electrostatic ion cyclotron waves excited by field-aligned currents.

1. Introduction

In the auroral zone ionosphere, electric field fluctuations accompanied by electron density fluctuations have been measured on many rockets and satellites (*e.g.* KELLEY and MOZER, 1973; BERING *et al.*, 1975; KINTNER *et al.*, 1978). These fluctuations are thought to be due to plasma waves of the electrostatic mode. Since the electron-neutral and ion-neutral collisions are predominant in the altitude range lower than ~140 km ion acoustic waves can be excited when the DC electric field is sufficiently large (usually greater than 30 mV/m). This type of plasma instability is called the two-stream instability (FARLEY, 1963). If the electron density gradient perpendicular to the geomagnetic field line has a parallel component to the direction of the DC electric field, another type of waves can be excited by much smaller DC electric fields (SATO, 1971). This type of instability is called the cross-field instability. The ion

acoustic waves and drift waves which are probably excited by these kinds of instabilities have been measured on sounding rockets (*e.g.* KELLEY and MOZER, 1973).

In the higher altitude region where the collision frequency is low, another type of plasma waves called the electrostatic ion cyclotron (EIC) waves becomes important. The excitation of the EIC waves on the auroral field lines has been studied from the interest of seeking for a possible acceleration mechanism of auroral particles. KINDEL and KENNEL (1971) examined the condition for the growth of the EIC and ion acoustic waves caused by field-aligned currents in the topside ionosphere. They found that the critical value of the field-aligned current for the excitation of the EIC wave is much smaller than that of the ion acoustic wave, and the heavy ion cyclotron wave is more easily excited than the light ion cyclotron wave in the lower altitude range. Their theoretical prediction has been partly confirmed by *in situ* observations on rockets and satellites. The S3-3 satellite has detected electrostatic waves, which are thought to be the H^+ EIC mode, on the auroral field lines at the altitude of $\sim 1 R_E$ (KINTNER *et al.*, 1978), while BERING *et al.* (1975) have suggested that the EIC wave of heavier ion (O^+) was detected on a sounding rocket near the equator edge of an auroral arc at the altitude of ~400 km.

A sounding rocket equipped with double-probes for electric field measurement was launched from Syowa Station, Antarctica around the onset time of an intense auroral substorm. Several kinds of electric field fluctuations were measured on the rocket when the rocket moved across an active auroral arc. In this report, the characteristics of these fluctuations are examined first, and then the modes of these fluctuations are discussed.

2. Instrumentation

Electric field fluctuations were measured on the rocket by a double-probe type detector with two spherical probes (diameter 4 cm) apart a distance of 2.45 m. The

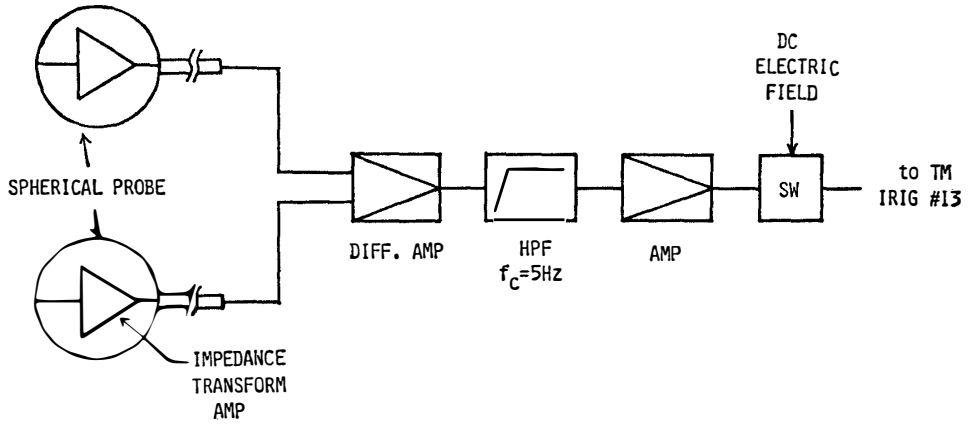

Fig. 1. Block diagram of the AC and DC electric field detector aboard the S-310JA-7 rocket.

DC electric field was also measured by using the same probes (OGAWA *et al.*, 1981). Both data were alternatively telemetered *via* IRIG FM channel, *i.e.*, two sedonds for AC electric field and six seconds for DC electric field. Fig. 1 shows the block diagram of this instrument. The range of the frequency response of this instrument is 5–220 Hz. The other items of the measurements of this rocket are electron density fluctuations in the ELF and VLF ranges, plasma waves from 0.1 to 8 MHz, auroral energetic particles in the low (below 105 eV) and medium (0.1–10 keV) energy ranges, electron density and electron temperature, as will be found in other papers in this issue.

3. Experimental Results

The S-310JA-7 rocket was launched geomagnetically northward from Syowa Station (geomagnetic latitude, 70.0°; longitude, 79.4°; $L=6.1$) at 191550 UT on March 27, 1978. An intense auroral substorm started at the equatorward of Syowa Station just before the launching time. Ground-based observation data concerning geomagnetic field variation, cosmic noise absorption, VLF emissions, and auroral

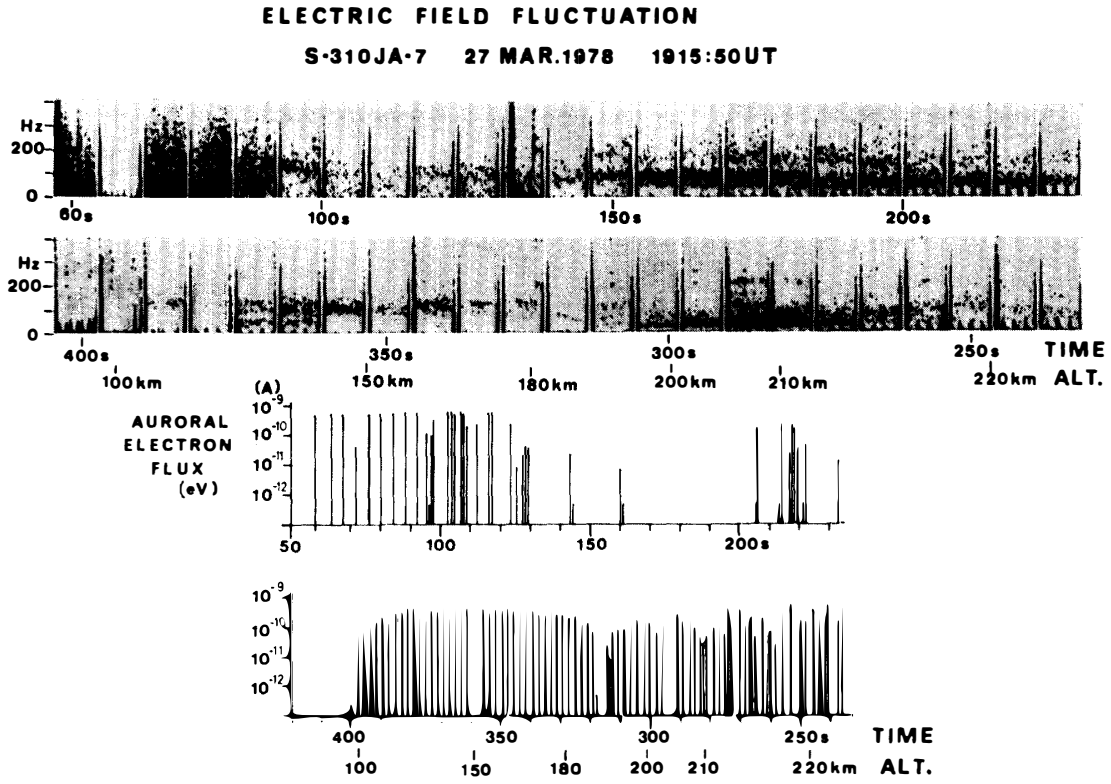

Fig. 2. F-t diagram of electric field fluctuations (upper two pannels). Auroral particle flux observed on the same rocket is also shown at the bottom.

motion during the rocket flight are shown in the paper by OGAWA *et al.* (1981) in this issue.

Presented in the upper two pannels of Fig. 2 are frequency-time (*f-t*) diagrams of the observed electric field fluctuations. Since the observation was carried out in accordance with the time-sharing program (two seconds for AC electric field measurement and six seconds for DC electric field measurement), each column of the pannel shows the *f-t* spectrum for two seconds, while the space between the two adjoining columns indicate the data gap for six seconds. The upper and lower *f-t* diagrams correspond to the ascent and the descent of the rocket flight, respectively. It should be noted that the time sequence of the lower pannel is inverted from right to left, so as to align the two *f-t* spectra observed at the same altitude. Plotted at the bottom in Fig. 2 are the auroral particle fluxes observed on the same rocket by OGAWA *et al.* (1981).

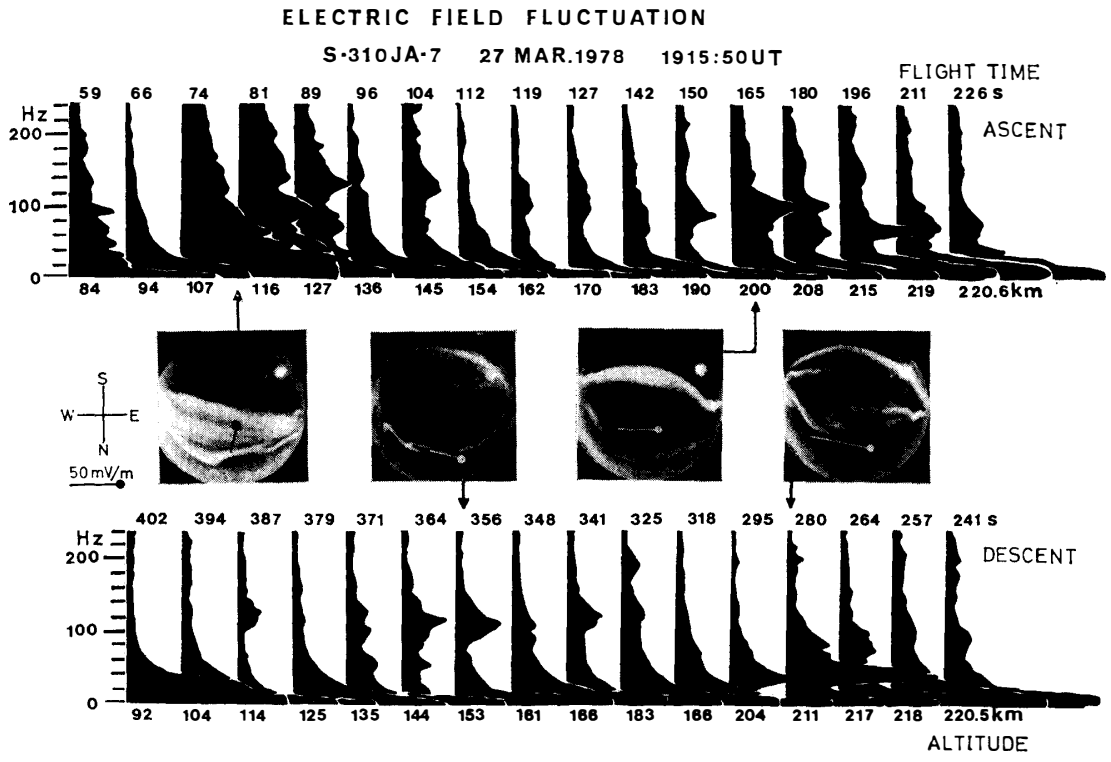

Fig. 3. Power spectra of electric field fluctuations. All-sky camera photographs of aurora with observed DC electric field are also shown at the middle.

Fig. 3 shows the sections of the *f-t* diagrams of electric field fluctuations at every 8 or 16 s during the rocket flight time. These power spectra are displayed on a linear scale. Each power spectrum represents the average for 5.6 ms by super-

imposing 16 power spectra calculated by the 256 point FFT method, having been sampled during two seconds of observation time. The numbers at the top and the bottom of each section indicate the flight time after launch in seconds and the rocket altitude, respectively.

The four all-sky camera photographs at the middle show the auroral forms, particularly in the time intervals when the strong electric field fluctuations were observed. The rocket position and the observed DC electric field are also shown in the photographs. The intense frequency component below 20 Hz in the power spectra in Fig. 3 originated from low-frequency noise bursts which are clearly seen at the bottom of the *f-t* diagram in Fig. 2. Note that these noise bursts arose twice during one spin period of 1.1 s. Therefore, it is thought that these are due to rocket-caused artificial disturbances probably in the wake of the rocket. Based on the *f-t* diagrams presented in Figs. 2 and 3, characteristics of the electric field fluctuations are summarized as follows.

3.1. Electric field fluctuations during the flight time 65–90 s (93–128 km)

As is shown in Fig. 9 in the paper by OGAWA *et al.* (1981), the rocket plunged into a poleward expanding auroral arc at around 65 s during the ascent. During the flight time of 65–67 s (93–96 km), significant electric field fluctuations were not observed, while during the flight time of 73–90 s (105–128 km), intense (1.4 mV/m) electric field fluctuations with a broadband structure were observed. The observed DC electric fields at these altitudes were directed magnetically northward with the intensity between 35 mV/m at the altitudes of 95 km and 20 mV/m at the altitude of 115∼128 km. The relative drift velocity V_d of electrons to that of ions caused by these electric fields lies between 780 m/s at 95 km and around 40 m/s at 115∼128 km. The observed electron temperature at these altitudes ranged from 400 K to 700 K, gradually increasing with the altitude (K. OYAMA, private communication). Therefore, the sound velocity C_s is estimated to be 350–500 m/s.

From the above estimations it is concluded that the condition for the two-stream instability is attained in the lower altitude range below 110 km, because V_d exceeds C_s. As the altitude increases, the condition for the two-stream instability breaks down at the altitude greater than 115 km. Nevertheless, the cross-field instability can grow if the electron density gradient parallel to the electric field exists. Therefore, it is likely that the fluctuation during 73–75 s (105∼108 km) is due to the ion sound wave generated by the two-stream instability, while the fluctuation during 80–90 s (115∼128 km) is due to the ion drift wave generated by the cross-field instability.

It is important to note that significant fluctuations of the electric field were not observed during 65–67 s (93–96 km), though the DC electric field was strong enough to cause the two-stream instability. Other rocket observations (HOLTET, 1973; OGAWA *et al.*, 1979) reported similar results that electric field fluctuations were observed only at the altitude higher than 95 km. The Hall effect becomes not efficient in such

low altitude range and it may be the reason why the instability is suppressed in the altitude range lower than 95 km.

3.2. Electric field fluctuations during the flight time 150–235 s (189–221 km)

The fluctuations of the electric fields which are characterized by the spectral structure with a narrow (20 Hz) bandwidth were observed during 150–235 s. The midfrequency trends to decrease from 100 Hz at 150 s to 70 Hz at 235 s. However, the associated fluctuation of electron density was not observed during this flight time. The rocket was located 100–180 km equatorward of a poleward moving arc, as shown in Fig. 3. The observed flux of precipitating electrons was small during this period.

The relative velocity between ion and electron drifts becomes small in this altitude range, since the collision frequency between charged particles and neutral particles decreases. Therefore, both the two-stream type and cross-field type instabilities are suppressed. The small amount of electron flux observed on the rocket seems to be insufficient for the current driven instability. However, the energy range of the observed electron flux was greater than 105 eV. Therefore, there is a possibility that the electron flux in the energy lower than 105 eV was enough to drive the EIC instability during this period.

3.3. Electric field fluctuations during the flight time 270–296 s (214.4–203 km)

The rocket was located equatorward of an auroral arc with a spiral structure. The power spectra of the electric field fluctuation showed a narrow-band structure with band-width of 10 Hz and a center frequency of 42 Hz. The peak value of the amplitude was 0.8 mV/m (r.m.s. value) at 279–281 s (211.4–210.5 km). The local ion gyro-frequency of O^+ was estimated to be 38 Hz at these altitudes, which is a little lower than the center frequency of the electric field fluctuation. The retarding potential analyzer on board observed strong electron flux of 10^8 electrons/cm^2•s around these times (OGAWA *et al.*, 1981). Thus, this fluctuation is expected to be the wave excited by the field-aligned electron flux.

If this fluctuation is due to the EIC wave, it is suggested that the fluctuation propagates in the plane perpendicular to the magnetic field. The phase velocity of the EIC wave can be estimated by means of the linear instability theory which gives a growth rate peaks at the perpendicular wave number k given by the relation $(k\rho_i)^2 = 1.5$, where ρ_i is the ion Larmour radius (KINDEL and KENNEL, 1971). Since the ion temperature was not measured on this rocket, a value of 1000 K is assumed as a typical ion temperature at the altitude of 200 km in the auroral ionosphere (*e.g.* ROBLE and REES, 1977). Then ρ_i becomes 3 m and the phase velocity is estimated to be 600 m/s. This is comparable to the rocket velocity component perpendicular to the magnetic field line, and also the $E \times B$ drift velocity of plasma, which are estimated to be 920 m/s and 1200 m/s, respectively. Therefore, the frequency of the electric field fluctuation in the rocket frame should be affected greatly due to the Doppler shift.

Considering this Doppler shift, NO^+ becomes one of the possible ion species which are responsible for the EIC wave, although the observed frequency is close to the O^+ gyro-frequency. A more quantitative discussion will be given in the next section.

Fig. 4 shows the telemetry-output wave form of the fluctuation observed during 278.8~280.7 s, which consists of almost a monochromatic wave of about 40 Hz with its amplitude showing a complicated variation. If a plane wave with a constant amplitude and a wavelength much longer than the antenna size is measured by the detector on board the rocket, the envelope of the output signal from the spinning antenna should show a sinusoidal variation with two null points during one spin period. The observed variation, however, seems to consist of two kinds of periodic components, *i.e.*, ~550 ms (half spin period) and 200 ms. Associated null points for both components are marked in Fig. 4, by bold and thin arrows, respectively. This result suggests the existence of a kind of spatial beat effect among multiple waves.

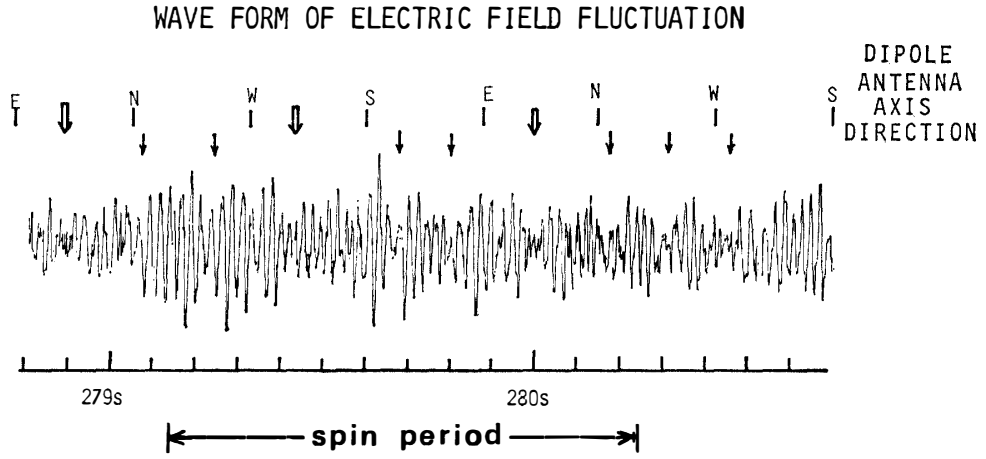

Fig. 4. Telemetry-output wave form of electric field fluctuation during 278.8–280.7 s.

3.4. Electric field fluctuations during the flight time 324–372 s (183.6–133.8 km)

Narrow-band fluctuations with a mid-frequency of about 120 Hz were observed at the flight time 324–372 s. The 60 Hz component also appeared during 363–372 s (144.8–133.8 km). The rocket was located at the equator-side of a equatorward drifting auroral arc, and the energetic electron flux with intensity of 10^8 electrons/$cm^2 \cdot s$ was observed during 324–372 s. Considering the intense electron flux and the narrow-band structure of the power spectra, it is suggested that the current-driven EIC instability is a possible mechanism for this fluctuation. However, the observed frequency is quite different from the gyro-frequencies of O^+ or NO^+ ions. As is mentioned above, it seems that the Doppler effect is important again to understand this frequency.

4. Discussion

In order to understand the meaning of the observed frequency of the narrow-band fluctuations, the Doppler effect should be considered, as mentioned in the previous section. As the first step the plasma flow velocity component perpendicular to the geomagnetic field in the rocket frame has been calculated by the following relation.

$$\vec{V}_{PR}=\vec{E}\times\vec{B}-\vec{V}_R \tag{1}$$

where $\vec{E}$, $\vec{B}$, $\vec{V}_R$ denote the DC electric field, the geomagnetic field, and the rocket velocity component perpendicular to the geomagnetic field, respectively. The magnitude of the plasma flow velocity $|V_{PR}|$ and its direction in the plane perpendicular to the geomagnetic field line are shown in Fig. 5 as a function of the flight time. As the second step, by using these values, the Doppler-shifted frequency f_{obs} of the wave in the rocket frame is given as

$$\begin{aligned} f_{obs} &= f_o \frac{1}{2\pi}\vec{k}\cdot\vec{V}_{PR} \\ &= f_o + \frac{1}{2\pi}|\vec{k}|\cdot|\vec{V}_{PR}|\cos\delta \end{aligned} \tag{2}$$

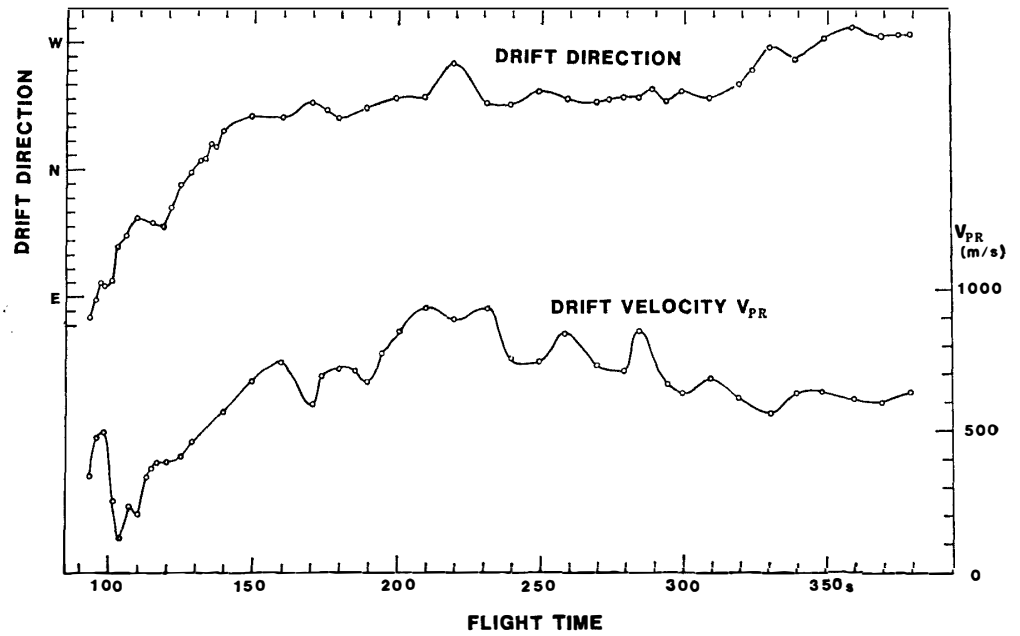

Fig. 5. Time variation of the direction of relative velocity between the rocket and plasma (upper line), and its absolute value (lower line).

where f_o denotes the wave frequency in the plasma frame and δ denotes the angle between $\vec{k}$ and $\vec{V}_{PR}$. From the linear instability theory (*e.g.* KADOMTSEV, 1966), f_o is estimated to be $1.2 f_H$ for $Te \simeq Ti$, and $\vec{k}$ is estimated from the relation $\vec{k}^2 \cdot \rho_i^2 = 1.5$, where ρ_i is calculated from the model ion temperature profile shown in Fig. 6. The Doppler shift due to the second term in eq. (2) varies as a function of δ. Its maximum value is attained when $\delta = 0$ ($\vec{k}$ is parallel to $\vec{V}_{PR}$).

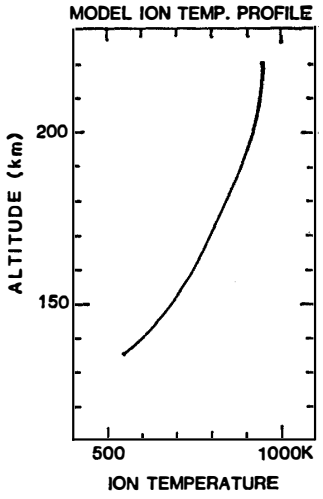

Fig. 6. Model ion temperature profile in the auroral ionosphere.

Fig. 7 shows $1.2 f_H$ for O^+ and NO^+ ion (dashed line) and the time variation of their upper limit of the frequency shift (hatched curves), which is attained when $\delta = 0$. The -3 dB band-width of the observed electric field fluctuation frequency is also shown by rectangles in Fig. 7. The hatched rectangles indicate narrow-band fluctuations with strong signal intensity. The fluctuations between 150 s and 235 s consist of two bands. The fundamental band is observed at $\sim$60 Hz, while the second band is observed at $\sim$80–110 Hz. Here it is apparent that the variation of the center frequency of the fundamental band is similar to the variation of the Doppler shift. Therefore, it seems to support the assumption that the observed fluctuations are due to the Dopper-shifted EIC wave. Since the frequency of the fundamental band is included in the upper limit of the Dopper-shifted frequency for NO^+, this band is explained by either O^+ or NO^+ EIC wave.

Fluctuations during 270–296 s can be explained again by either O^+ or NO^+ EIC wave. If the O^+ EIC wave is assumed, δ should be 96° and $\vec{k}$ should point the geomagnetically NE or SWS direction. In the case of the NO^+ EIC wave, δ should be 66° and $\vec{k}$ should point the NNE or WSW direction. As for the fluctuation observed after 332 s, the frequency is too high to be explained by the O^+ or NO^+ EIC wave, if this fluctuation is due to a fundamental band. Under the condition that $T_e \gg T_i =$ 300 K, the frequency of the EIC wave is expected to be $1.5 f_H$. The upper limit of

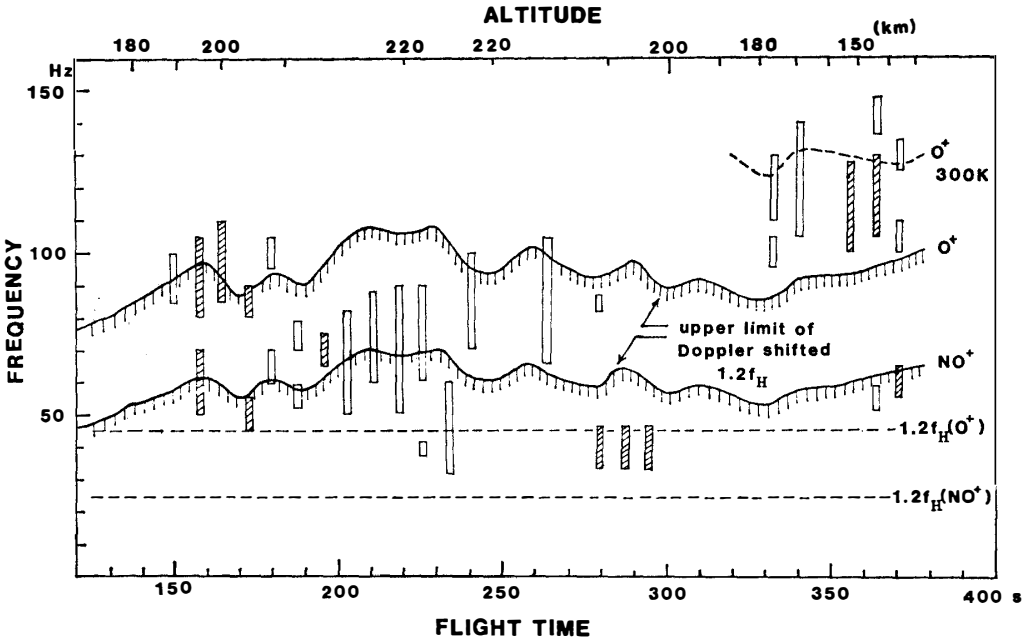

Fig. 7. Expected frequency of O^+ and NO^+ EIC wave (dashed line) and the time variation of the upper limit frequency of the Doppler shifted EIC wave in the rocket frame. The −3 dB band-width of the observed electric field is also shown by rectangles. The hatched rectangles indicate fluctuations with strong signal intensity.

the Doppler shift for this wave is shown as a dashed line near 130 Hz, but such a condition seems to be difficult in this altitude range. Therefore, this fluctuation may be due to the Doppler shifted second harmonic of the O^+ EIC wave, since the low frequency component about 60 Hz was also observed during 363–372 s. Neverthless, it should be explained why the second harmonic wave grows stronger than the fundamental wave in this case.

5. Conclusion

When the S-310JA-7 rocket was launched into highly active auroras, various kinds of electric field fluctuations were observed in the frequency range from 5 Hz to 220 Hz. The following is the summary of the observed facts and generation mechanism.

(1) Wide-band fluctuations with the maximum amplitude of 1.4 mV/m were observed in a highly active auroral arc in the altitude range of 105–128 km. At the altitude of 105∼108 km, the intense (30 mV/m) DC electric field was observed. Therefore, this fluctuation can be considered as ion sound waves caused by the two-stream instability. Since the DC electric field was too weak for the two-stream instability in the altitude range of 115–128 km, the cross-field instability should be considered for this fluctuation.

(2) Narrow-band fluctuations with a band-width of ~10 Hz and a center frequency of 42 Hz are observed in the altitude range of 214.4–203 km. The amplitude fluctuation reached 0.8 mV/m. Strong fluxes of precipitating electron were observed at this time. Therefore, this fluctuation seems to be electrostatic ion cyclotron waves of the O^+ or NO^+ mode excited by field-aligned electron fluxes.

(3) Narrow-band fluctuations with 70 Hz–100 Hz frequency were observed in the altitude range of 189–221 km during the ascent. The narrow-band fluctuations around 60 Hz and 120 Hz were observed at 184–134 km during the descent. It is likely that these are due to the Dopper-shifted EIC waves of O^+ or NO^+ ions.

Acknowledgments

We wish to express our thanks to the members of the 19th wintering party of the Japanese Antarctic Research Expedition for their kind effort in launching rockets and for their data acquisition of ground based geophysical observations.

We are also grateful to Dr. T. OGAWA of the Radio Research Laboratories for his helpful discussions about plasma instability in the ionosphere, and for presenting us with the data of auroral particle fluxes and electron density fluctuations observed by the same rocket.

References

CERING, E. A., KELLEY, M. C. and MOZER, F. S. (1975): Observations of an intense field-aligned thermal ion flow and associated intense narrow band electric field oscillations. J. Geophys. Res., **80**, 4612–4620.

FARLEY, D. T. (1963): A plasma instability resulting in field-aligned irregularities in the ionosphere. J. Geophys. Res., **68**, 6083–6097.

HOLTET, J. A. (1973): Electric field microstructures in the auroral *E* region. Geophys. Norw., **30**, 1-88.

KADOMTSEV, B. B. (1965): Plasma Turbulence. New York, Academic Press.

KELLEY, M. C. and MOZER, F. S. (1973): Electrid field and plasma density oscillations due to the high-frequency Hall current two-stream instability in the auroral *E* region. J. Geophys. Res., **78**, 2214–2221.

KINDEL, J. M. and KENNEL, C. H. (1971): Topside current instabilities. J. Geophys. Res., **76**, 3055–3078.

KINTNER, P. M., KELLEY, M. C. and MOZER, F. S. (1978): Electrostatic hydrogen cyclotron waves near one earth radius altitude in the polar magnetosphere. Geophys. Res. Lett., **5**(2), 139–142.

OGAWA, T., MORITA, M., FUKUNISHI, H., MATSUO, T. and YOSHINO, T. (1979): Nankyoku roketto S-210JA-24, 25-gôki ni yoru denrisô denba no kansoku (Measurements of ionospheric electric fields with Antarctic sounding rockets S-210JA-24 and 25). Nankyoku Shiryô (Antarct. Rec.), **63**, 252–275.

OGAWA, T., MORI, H., MIYAZAKI, S. and YAMAGISHI, H. (1981): Electrostatic plasma instabilities in highly active aurora observed by a sounding rocket S-310JA-7. Mem. Natl Inst. Polar Res., Spec. Issue, **18**, 312–329.

ROBLE, R. G. and REES, M. H. (1977): Time-dependent studies of the aurora: Effects of particle precipitation on the dynamic morphology of ionospheric and atmospheric properties. Planet. Space Sci., **25**, 991–1010.

SATO, T. (1971): Non-linear theory of the cross-field instability, explosive mode coupling. Phys. Fluids, **14**, 2426–2435.

(Received October 17, 1980; Revised manuscript received January 17, 1981)